Structure of Cubic Insulin Crystals in Glucose Solutions

Bin Yu and Donald L. D. Caspar
Institute of Molecular Biophysics, Florida State University, Tallahassee, Florida 32310 USA

ABSTRACT X-ray structures of cubic insulin crystals in high concentrations of glucose at different pH levels and temperatures have been refined to high resolution. We have identified one glucose-binding site near the N-terminus of the A-chain whose occupancy is pH dependent. The effects of reduced water activity on the ordered protein and solvent structures have been examined. Our analysis showed no notable conformational changes in the ordered protein structures or ordered solvent molecules near the protein surface, but the presence of glucose does have a significant effect on the overall density distribution of the bulk solvent in the solvent-accessible volume. We compared the structure of cubic insulin at room temperature and liquid-nitrogen temperature, under identical solvent conditions, using glucose as a cryoprotectant. In this case, we found that the average temperature factor of the protein is reduced and more water molecules can be identified, but there are no significant changes in the protein conformation.

INTRODUCTION

Insulin is a 51-amino-acid hormone that regulates the glucose level in blood. Deficiency in secretion or action of insulin in response to the level of glucose causes an abnormally high concentration of sugar, which can have profound impacts on metabolism in the human body. Major complications found in diabetics include high glucose levels in blood and urine, excessive excretion of urea, decrease in blood pH levels, inability to convert excessive glucose into triacylglycerol, and incomplete but excessive oxidation of fatty acids in the liver. The important biochemical role insulin plays in the metabolism of carbohydrates and the widespread occurrence of diabetes have made insulin one of the most extensively researched molecules.

The insulin molecule consists of two peptides: A and B, covalently linked by two disulfide bonds, and containing 21 and 30 residues, respectively. Native insulin crystallizes in cubic, monoclinic, and rhombohedral space groups in dimeric form. The 2-zinc rhombohedral form has been determined to 1.5-Å resolution (Baker et al., 1988). The cubic zinc-free form has been resolved to 1.7 Å (Badger et al., 1991). In both cases, the structure of the insulin dimer has been carefully refined and extensively analyzed.

The cubic form of insulin crystallizes in the absence of Zn ions (space group $I2_13$, $a = 78.9$ Å). It has much larger solvent content (64%) and diffracts to somewhat lower resolution than the rhombohedral 2-Zn form, which contains only 35% solvent by volume. The insulin dimers in the cubic crystal are arranged in orthogonal rows, which form large solvent channels. Thus a significant volume of the crystal is accessible by the "bulk" solvent. Because of its large solvent content and stability, the cubic insulin crystal provides a model system for exploring protein-solvent interactions under a wide range of conditions. The cubic crystal is stable from pH 5 to pH 11, and in salt concentrations from 0.1 M to 1 M (Gursky et al., 1992). At pH 7, ~30% of its residue conformations are different from those in the pH 11 form. Some of the pH-dependent discrete conformational changes involve water molecules directly. A dramatic example of the central role of solvent in the crystal is allosteric ion binding, which is mediated through a network of water molecules spanning almost the entire asymmetrical unit (Gursky et al., 1994, and manuscript submitted for publication). It is therefore interesting to explore the behavior of insulin in high concentrations of glucose, where water activity is reduced.

MATERIALS AND METHODS

Crystallization of cubic Zn-free insulin

The following recipe was prepared by Dr. Olga Gursky, who also generously supplied many of the crystals used in the experiments:

1. Bovine insulin powder from Sigma Chemical is dissolved to 18 mg/ml in an aqueous solution containing 0.05 M Na_2HPO_4, 0.001 Na_3EDTA. The pH is adjusted to 11.0, and the solution is left standing for 30 min and then filtered through a 0.22 Millipore filter.
2. A dialysis solution containing 0.12 M Na_2HPO_4 and 0.001 Na_3EDTA is buffered at pH 9.0.
3. The insulin solution is placed in 35–50-μl dialysis buttons sealed with 1000 MW dialysis membranes. Buttons are then left in the dialysis solution for 12–24 h.
4. Saturated Na_2HPO_4 solution is then added to adjust the final salt concentration to ~0.3 M. The final pH is ~9.2.
5. Cubic insulin crystals appear in ~24 h.

Data collection and structure refinement

Because crystals are grown in buttons covered with dialysis membranes, it is quite convenient to change the buffer conditions through many steps of dialysis. The concentration of glucose is adjusted by transferring dialysis buttons to buffers of successively higher concentrations of glucose, while keeping the ion concentration identical. Crystals are found to be stable in concentrations up to saturation (3 M D-glucose in pyranose form). Sugars have been known to stabilize protein in solution and enhance protein associations. In our case, the addition of glucose seems to contribute to a significantly longer shelf life of the crystals.

For room temperature data collection, crystals were mounted in capillaries. Crystals for cryo-data collection were mounted in fiber loops on top of fiberglass pins. The typical dimensions of the crystals are between 0.5 mm and 1.0 mm. Only one crystal was used for each data set. We collected data on crystals in buffers from pH 5 to pH 10 at room temperature, and crystals at pH 9 at liquid nitrogen temperature, as summarized in Table 1. With the exception of the tungstate-containing crystal, on which data were

TABLE 1 Statistics and conditions of data collection

pH	Salt	Sugar (M)	Detector	Resolution (Å)	Completeness (%)	R_{merge} (%)
5.2	1 M SO_4	2	Raxis-B*	1.82	94	5.4
5.7	0.25 M HPO_4	2	Raxis-F[#]	1.9	94	5.5
9[§]	1 M WO_4	2	Mar[¶]	2.9	100	3.4
9	0.25 M HPO_4	2	Raxis-F	1.88	94	5.8
9[§]	0.25 M HPO_4	2	Xentronics[‖]	2.0	99	5.4
9	0.25 M HPO_4	1	Raxis-B	2.0	95	4.5
10	0.25 M HPO_4	2	Raxis-B	1.83	90	6.0

$$R_{merge} = \frac{\sum_H \sum |I_i(H) - \langle I(H)\rangle|}{\sum_H \sum I_i(H)}$$

where $I_i(H)$ and $\langle I(H)\rangle$ are the ith measurement and mean value of the intensity of reflection H.
*RAXIS-B: Brandeis RAXIS imaging-plate detector.
[#]RAXIS-F: RAXIS-II imaging-plate detector at Florida State University.
[§]Cryo-data collected at 160 K. All other sets were collected at room temperature.
[¶]Mar: Mar Imaging plate detector at beam-line x12c, Brookhaven National Laboratory.
[‖]Xentronics: Multiwire area detector at Harvard University.

collected with synchrotron radiation at 1.215 Å, all other data sets were collected using Cu-Kα radiation at 1.5418 Å. Data were integrated and merged with DENZO and SCALEPACK (Otinowski, 1990), except for the data set collected on the Xentronics at Harvard, which was processed with the Harvard data-processing package and merged with the CCP4 suite of programs (Collaborative Computing Project Number 4, 1994).

The reference model for all refinements of the glucose-containing crystals was based on the model of the cubic pig insulin crystal at pH 9 in 0.2 M phosphate buffer that was refined to 1.7 Å resolution (Badger et al., 1991). Bovine insulin, the sequence of which differs from that of pig insulin at residues A8 and A10, has a virtually identical structure for the conserved residues in cubic crystals at pH ~9 in 0.1–1 M salt solutions (Gursky et al., 1992). In the initial model of the glucose-free cubic bovine insulin crystal, only 16 well-ordered water molecules ($B < 40$ Å^2) were kept from the 81 in the previously refined structure.

Refinement of high-resolution models was carried out with X-PLOR 3.1 (Brunger, 1992b) and TNT (Tronrud, 1992; Tronrud et al., 1987). The basic steps of refinement are summarized as follows. One starts with several rounds of conjugate gradient minimization and simulated annealing refinement of the starting model using X-PLOR. The good quality of the starting model usually allows the refinement of the initial model to proceed in an automatic fashion to very agreeable numbers. That leaves a relatively small amount of manual model-rebuilding using computer graphics (Jones et al., 1991), which mostly involves checking the density of disordered side chains, the possible density of glucose molecules, and positions of newly added water molecules. The model-building stage ends when no more water molecules can be located or no more meaningful reduction in R_{free} can be achieved (Brunger, 1992a). Finally, TNT least-square refinement is used to complete the structure refinement. The refinement statistics for five glucose-containing crystals at pH 5.7, 9, and 10 are summarized in Table 2.

RESULTS AND DISCUSSION

Changes in protein structure

Because there are some small differences in the unit-cell parameters, refined atomic models were first superimposed on each together as a way of trying to minimize the least-squares difference between the main-chain atoms. Table 3 shows the RMS difference in atomic positions between the refined models for glucose-containing crystals and the reference model for the glucose-free crystal at pH 9 after the superimposition. It is quite obvious that all refined models correlate well with the original model, and the mean difference in atomic positions is within the uncertainty estimated from Luzzati statistics (Luzzati, 1952) of the models themselves. The RMS difference of individual residues also showed little correlation with the glucose concentration (Fig. 1). Thus overall conformations of cubic insulin are very similar at glucose concentrations of up to 40% weight.

In glucose-free crystals at any pH, side chains of B21 Glu, B29 Lys, and the C-terminus of the B-chain (B30 Ala)

TABLE 2 Refinement statistics of glucose-buffered insulin crystals

Buffer conditions	R_{crys} (%)*	R_{free} (%)*	No. of waters	RMSD angle (°)[#]	RMSD bond Å[#]
pH 5.7, 2 M gluc.	16.3	20.7	35	1.6	0.010
pH 9.0, 1 M gluc.	16.5	21.8	31	1.8	0.011
pH 9.0, 2 M gluc.	17.2	22.2	37	1.8	0.011
pH 9.0, 2 M gluc., 160 K	16.6	23.7	81	2.0	0.014
pH 10.0, 2 M gluc.	17.1	21.8	33	1.7	0.009

$$R_{crys} = \frac{\sum_H \| F_{obs}(h)| - |F_{calc}(h)\|}{\sum_H |F_{obs}(h)|}$$

where obs and calc refer to observed and calculated structure factors, respectively.
R_{free}: Calculated from 10% of the data randomly chosen and omitted from the refinement.
[#]RMSD angle and bond: RMS deviation from ideal bond length and bond angles.

TABLE 3 Comparison of refined glucose-containing crystal structures with reference, glucose-free model

	pH 5.7 2 M gluc.	pH 9.0 2 M gluc.	pH 9.0 1 M gluc.	pH 9.0 cryo 2 M gluc.	pH 10 2 M gluc.
RMS Cα position (Å)	0.23	0.18	0.19	0.21	0.20
RMS positions (all atoms)	0.40	0.28	0.34	0.41	0.38
Conserved waters*	24	16	24	37	20

*Conserved waters are defined as water molecules within 2 Å of a water molecule in the reference model.
RMS positions compare the positions of protein atoms only.

have multiple conformations and cannot be uniquely modeled (Gursky et al., 1992). A4 Glu is only uniquely ordered at pH < 7. These residues are all charged and have access to bulk solvent. In the glucose-containing structures, these residues do not show up any more clearly in the electron density map. Thus the presence of glucose does not seem to affect the conformational variability of very flexible residues.

The only major local change in the glucose-containing structure from the reference structure is a 0.8-Å shift of B1 Phe. The main-chain oxygen of B1 forms a hydrogen bond to Nε1 of B4 Gln. The involved residues tilted as a rigid body. The side chains of these residues did not adopt new conformations as a result of the overall shift. It also appears that B4 has only one conformation, as opposed to two conformations of equal occupancy in the reference glucose-free structure. No glucose molecules appear to be involved directly in the shift of B1 Phe.

Of all discrete pH-dependent conformational changes observed in the absence of glucose (Gursky et al., 1992), only the one involving A5 Gln, A9 Ser, and a pair of water molecules behaves differently. At pH 7 and low ionic strength, A5 and A9 adopt the "open" conformation (70% occupancy), pointing away from their symmetry mates. At pH 9 and above, they exist only in the "closed" conformation and displace two water molecules in the process. One expects the open conformation to have even higher occupancy at pH 5.7. That conformational switch does not happen in the presence of glucose. In the electron density map, one can recognize only the closed conformation. The occupancy should be close to 1, because the temperature factors of the side chains are similar to those of their respective main-chain atoms.

pH-dependent glucose binding at A1

At pH 10, there is a glucose molecule that binds strongly to the N-terminus of the A-chain (Fig. 2). The O5 atom in the glucose ring hydrogen bonds to the terminal nitrogen of A1

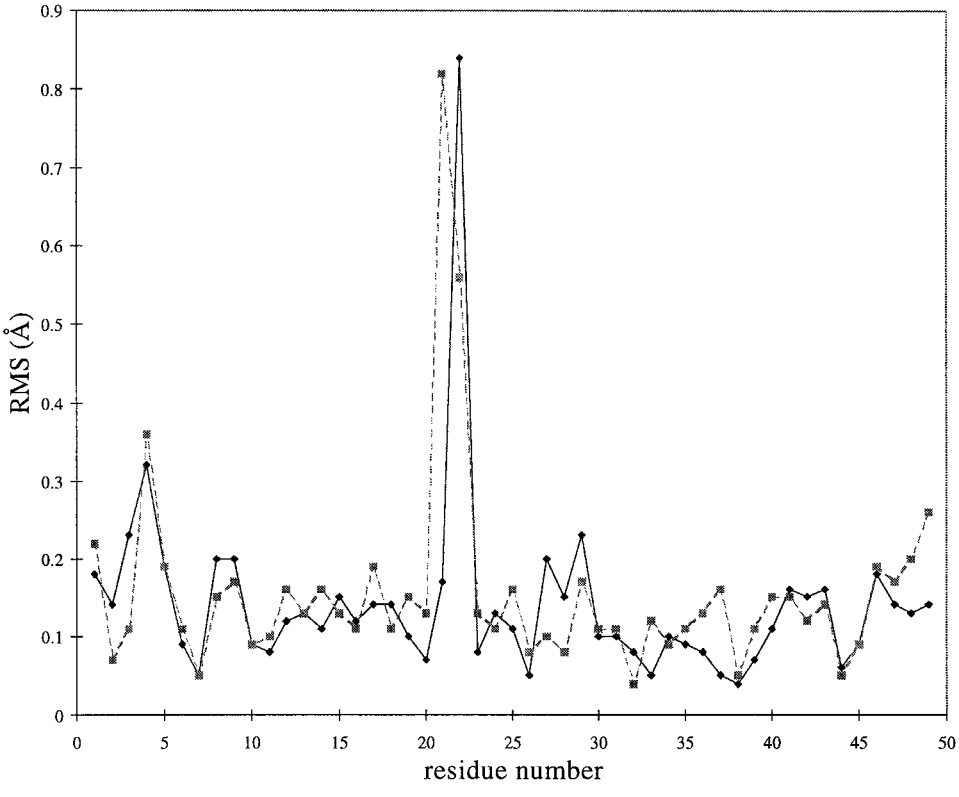

FIGURE 1 RMS differences in the refined Cα positions in crystals at pH 9 with 1 M glucose (*dashed line*) and 2 M glucose (*solid line*) compared to the reference, glucose-free crystal model. The Cα RMS differences are plotted as a function of residue number starting from A1 to B28 for a total of 49 residues. Because B29 and B30 are disordered in all crystals, their coordinates are not compared.

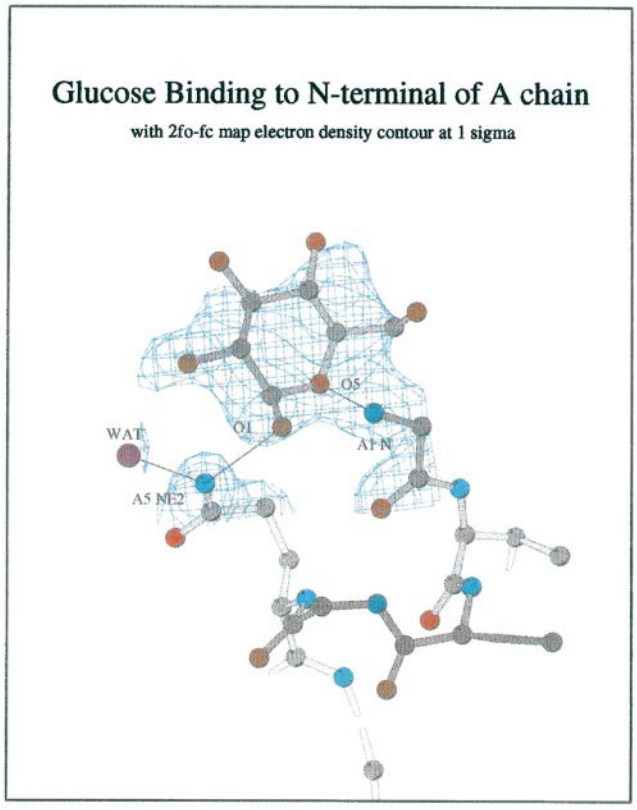

FIGURE 2 Glucose binding to A1 at pH 10. Protein atoms are shown as ball-and-stick models in the picture; electron density contour at 1 sigma is shown as a mesh. Created with Molscript (Kraulis, 1991).

Gly (distance 2.3 Å). O1 of glucose forms a hydrogen bond to Nε1 of A5 Gln. These are the only two points that connect glucose to the protein molecule, although the O-N interaction must be quite strong, because the glucose density in the map is connected to the protein density. The rest of the glucose molecule suspends freely in the solvent channel and has high mobility (temperature factors of these atoms hover around 100). Neither A1 nor A5 changed conformation to accommodate the glucose binding. It is quite remarkable that glucose can take advantage of an existing hydrogen-bonding network and dock very precisely into a crevice on the protein surface.

At pH 9, the electron density of the glucose is still connected but not nearly as clear. It becomes completely invisible at lower pH values. The pH dependence can easily be explained, because the pK value of A1 glycine's NH_3^+ group is 9.6. At less than pH 9.6, the A1-N is protonated, which favors hydrogen bonding with water molecules. As there is no other direct connection to the protein, the glucose molecule is less restrained and its density is unrecognizable.

Comparison of ordered solvent structure

Coordinates of 81 water molecules in the 1.7-Å glucose-free cubic insulin structure (Badger et al., 1991) were deposited with the Protein Data Bank. Our refined models, with the exception of the cryostructure, contain far fewer waters. This is due to the lower resolution at which data were collected, and the very conservative criteria we employed in locating water molecules, rather than to the presence of sugar. Of the 81 waters in the cryostructure, 37 are within 1.5 Å of a water identified in the glucose-free structure. The Debye-Waller factor is a measure of the root mean square deviation of the atomic position and thus is an indicator of the behavior of atomic motion. Fig. 3 shows a strong correlation in the temperature factors between conserved water molecules, which indicates that, on the average, the hydrogen bonding environment and arrangement of strongly bound solvents are not affected significantly by the differences in temperature and water activity.

As crystals are mounted into capillaries, they are often treated with dicholoroethane to prevent slippage during data collection. Dicholoroethane binds at half-occupancy in the pocket on the crystal dyad formed by B12 Val, B16 Tyr, and their symmetry mates (Gursky et al., 1994). The binding is conserved in the glucose-containing structure.

Density distribution of the bulk solvent

One can determine the density distribution of all solvents accurately from phased low-resolution data. We refined the phases of low-resolution reflections by using the difference map flattening protocol (Badger and Caspar, 1990; Jiang and Brunger, 1994; Yu, 1997). We computed the radial distribution function (RDF) of the solvent density of crystals in different ionic conditions and temperature, both in 2 M glucose (Fig. 4). The RDF of crystal buffered in 1 M tungstate at liquid nitrogen temperature is similar to that of crystals containing phosphate at room temperature. There-

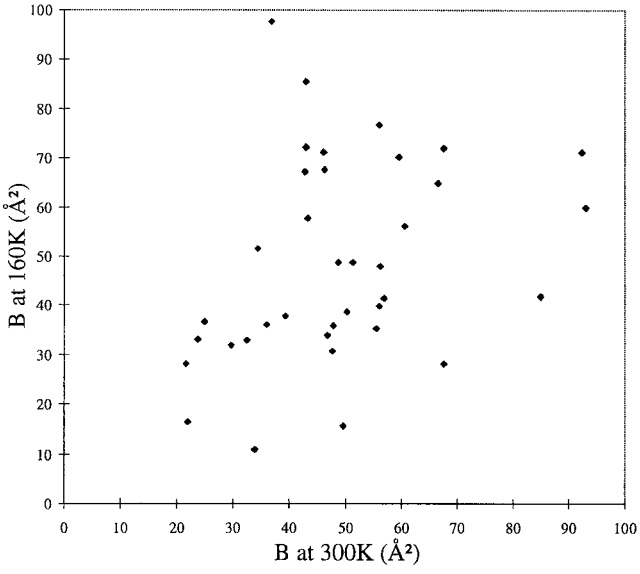

FIGURE 3 Covariance of water temperature *B* factors. The *B* factors (Å^2) of water molecules in the cryocrystal at 160 K in 2 M glucose are plotted against the *B* factors of 37 corresponding water molecules in the reference, glucose-free crystal at room temperature.

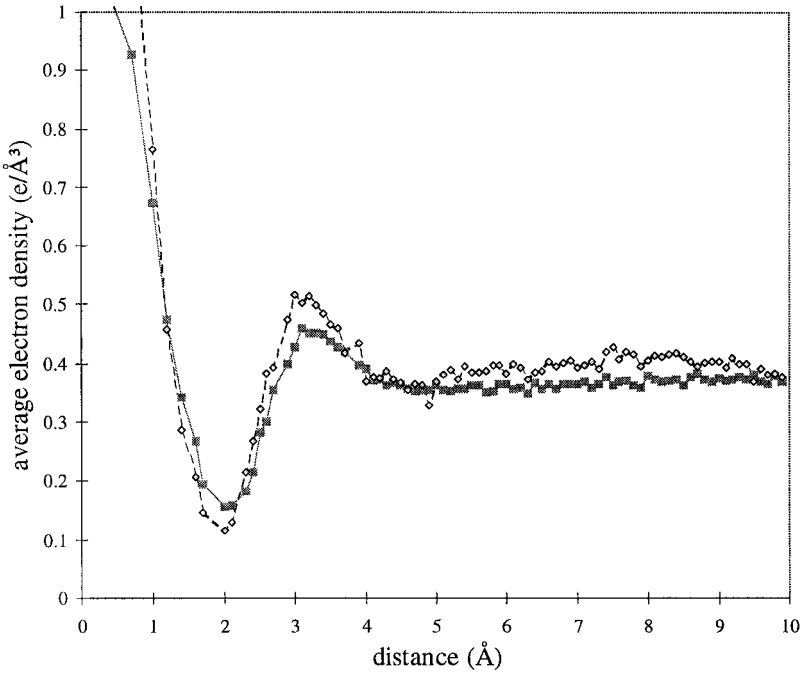

FIGURE 4 Averaged radial electron density distribution of solvent in cubic insulin as a function of distance from the protein surface for crystals in 2 M glucose, pH 9, one with 0.25 M phosphate at room temperature (*solid line*) and the other with 1.0 M tungstate at 160 K (*dashed line*). The electron density maps were calculated using all of the low-resolution data, which were phased by difference map flattening, and put on an absolute scale. The distance of each pixel in the maps is defined as the distance to the closest ordered protein atom. Densities at equal distances were averaged to produce these radial density distributions. Beyond ~5 Å from the surface, the mean electron density corresponds to that calculated from the solvent composition.

fore ion concentration, type of ions, and temperature of the buffer do not seem to effect the overall density distribution of the bulk solvent, although, as expected, the mean density is higher in the crystal with tungstate.

The strongest feature of the radial density profile is a broad peak between 3 and 4 Å, which represents the network of nonrandom distribution of water molecules, sugar, and ions near the protein surface. However, in the absence of a high concentration of sugar, one observes additional peaks of diminishing amplitude in the RDF, which were detected out to ~15 Å from the surface, corresponding to successive shells of hydration (Badger, 1993). In contrast, the density distribution beyond the surface layer in the glucose-containing crystals is relatively smooth because intermolecular interactions between waters needed to maintain an ordered network are disrupted by the large glucose molecules. As was found in the case of the glucose-free crystals (Badger, 1993), the first hydration shell, which includes both weakly and well-ordered solvent, is conserved, but the peak in the distribution with 2 M glucose is broadened and shifted to a slightly higher radius. Preferential hydration of protein is also observed in the subtilisin Carlsberg structure, where the bulk solvent is replaced by acetonitrile (Fitzpatrick et al., 1993).

Cubic insulin structure at low temperature

Glucose is a very effective cryoprotectant. A 2 M concentration of glucose is ~40% by weight, which is high enough for the solvent to form glass at liquid nitrogen temperature. This provides us with an opportunity to compare protein structures in a typical cryoprotectant under otherwise strictly identical solvent conditions at different temperatures. Previous studies on effects of temperature on protein structure relied on data collected for crystals soaked in different solutions at room and liquid nitrogen temperatures (Tilton et al., 1992), or without cryoprotectant (Frauenfelder et al., 1987; Hartmann et al., 1982).

The cubic unit-cell dimensions of a crystal frozen at 160 K decreased very slightly from 78.9 Å to 78.7 Å. This decrease is statistically significant, however, because variations from the unit-cell parameters of crystals at room temperature are always less than 0.1 Å, regardless of pH or ionic strength of the buffer. The unit-cell length of flash-frozen crystals can vary more significantly, depending on conditions. In another diffraction experiment on a flash-frozen crystal in 2 M glucose and 1 M tungstate (Yu, 1997), the unit-cell constant of a tungstate-soaked crystal indexed to 77.2 Å, indicating partial dehydration.

Comparison of the refined structures of cubic insulin crystals in 2 M glucose at 160 K and 300 K (Fig. 5) demonstrates that, except for the N-terminus of the A-chain and C-terminus of the B-chain, there are no differences in the Cα coordinates larger than expected for the statistical uncertainty in the refinement (Luzzatti, 1952). The A1 amino group is involved in the pH-dependent binding of glucose, and there may be some effect of temperature on this interaction. Residues B29 and B30 have very large temperature factors in the room temperature crystal due to positional disorder, and even though they are better ordered at low temperature, comparison of their mean positions is uncertain. Comparison of the average temperature factors of the amino acid residues in the crystals at 160 K and 300 K (Fig. 6) shows that the individual B factors are, in general,

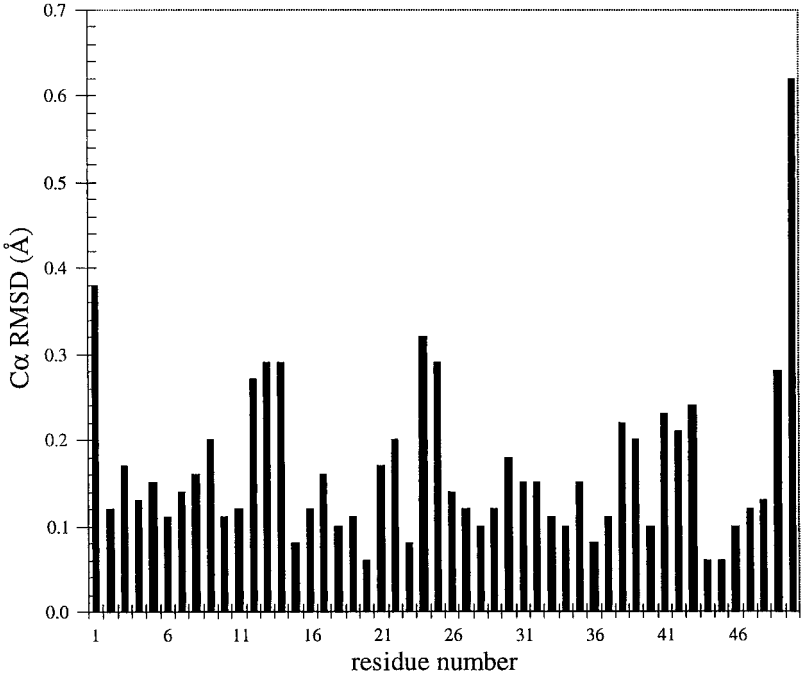

FIGURE 5 RMSD of Cα positions between 160 K and 300 K insulin in 2 M glucose. Note that these RMS deviations, except for A1 and B30, are on the order of the uncertainty in atomic coordinates expected from Luzzatti statistics.

systematically smaller at the lower temperature; and the average B factor for all protein atoms decreases with temperature from 34 $Å^2$ to 25 $Å^2$. Furthermore, at the low temperature, bound water molecules show up as sharper peaks in the electron density map; 81 ordered water molecules could be identified in the 160 K crystal map compared to 37 in the map for the crystal at 300 K (Table 2), even though the 160 K data were only collected to 2.0-Å resolution compared to 1.8-Å resolution for the 300 K data. Side chains that are positionally disordered at room temperature, however, remained disordered at low temperature. In conclusion, our comparison of the cubic insulin crystal structure at room temperature with and without glucose, and comparison of glucose-containing crystals at room and liquid

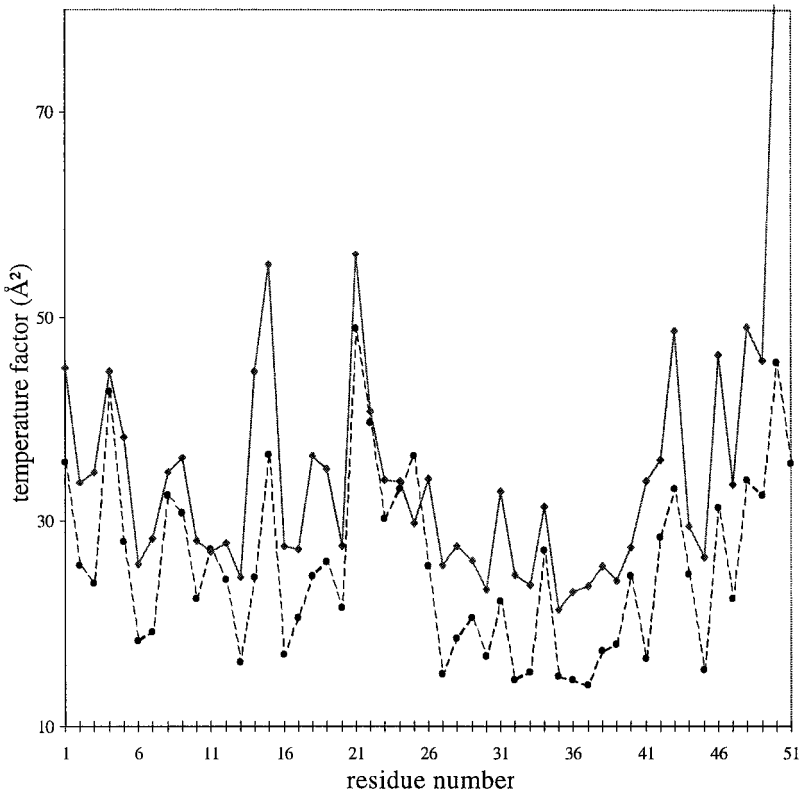

FIGURE 6 Average temperature *B* factors of ordered atoms in each amino acid residue for crystals in 2 M glucose at 160 K (*dashed line*) and 300 K (*solid line*). Residues are numbered from 1 to 51, starting from A1 through B30.

nitrogen temperatures demonstrate that the cryoprotectant has little effect on the ordered protein structure, and flash-freezing preserves the room-temperature structure with a small, but significant, reduction in the thermal fluctuations.

Atomic coordinates resulting from this work will be deposited with the Protein Data Bank.

Dr. Alex Kapulsky's work in the exploratory stage of this project is acknowledged. We thank Dr. Robert Sweet and his staff at Brookhaven National Laboratory, NSLS beamline X12c, for their help in collection the synchrotron data, and Dr. Stan Watowich for technical assistance on cryo-data collection at the Wiley-Harrison Laboratory, Howard Hughes Institute, Department of Biochemistry and Molecular Biology, Harvard University.

This work has been supported by U.S. Public Health Service Research grant CA47439 to DLDC from the National Cancer Institute.

REFERENCES

Badger, J. 1993. Multiple hydration layer in cubic insulin crystals. *Biophys. J.* 65:1656–1659.

Badger, J., and D. L. D. Caspar. 1990. Water structure in cubic insulin crystals. *Proc. Natl. Acad. Sci. USA.* 88:622–626.

Badger, J., M. R. Harris, C. D. Reynolds, and A. C. Evans. 1991. Structure of pig insulin dimer in the cubic crystal. *Acta Crystallogr.* B47:127–135.

Baker, E. N., T. L. Blundell, J. F. Cutfield, S. M. Cutfield, E. J. Dodson, G. G. Dodson, D. M. C. Hodgkin, R. E. Hubbard, N. W. Isaacs, C. D. Reynolds, K. Sakabe, N. Sakabe, and N. M. Vijayan. 1988. The structure of two Zn pig insulin crystals at 1.5 Å resolution. *Philos. Trans. R. Soc. Lond. Biol.* 319:369–456.

Brunger, A. T. 1992a. Free R value: a novel statistical quantity for assessing the accuracy of crystal structures. *Nature.* 355:472–475.

Brunger, A. T. 1992b. X-PLOR, Version 3.1. Yale University, New Haven, CT.

Collaborative Computing Project Number 4. 1994. The CCP4 suite: Programs for protein crystallography. *Acta Crystallogr.* D50:760–763.

Fitzpatrick, P. A., A. C. U. Steinmetz, D. Ringe, and A. M. Klibanov. 1993. Enzyme crystal structure in a neat organic solvent. *Proc. Natl. Acad. Sci. USA.* 90:8653–8657.

Frauenfelder, H., H. Hartman, M. Karplus, I. D. J. Kuntz, J. Kuriyan, F. Parak, G. A. Petsko, D. Ringe, R. F. J. Tilton, M. L. Connolly, and M. Nelson. 1987. Thermal expansion of a protein. *Biochemistry.* 26: 254–261.

Gursky, O., J. Badger, Y. Li, and D. L. D. Caspar. 1992. Conformational changes in cubic insulin crystals in the pH range 7–11. *Biophys. J.* 1992:1210–1220.

Gursky, O., E. Fontano, B. Bhyravbhatla, and D. L. D. Caspar. 1994. Stereospecific dihaloalkane binding in a pH-sensitive cavity in cubic insulin crystals. *Proc. Natl. Acad. Sci. USA.* 91:12388–12392.

Hartmann, H., F. Parak, W. Steigemann, G. A. Petsko, D. Ringe, and H. Frauenfelder. 1982. Comformational substates in a protein: structure and dynamics of metmyoglobin at 80 K. *Proc. Natl. Acad. Sci. USA.* 79: 4967–4971.

Jiang, J.-S., and A. T. Brunger. 1994. Protein hydration observed by X-ray diffraction. *J. Mol. Biol.* 243:100–115.

Jones, T. A., J. Y. Zou, S. W. Cowan, and M. Kjelgaard. 1991. O. (Ver. 5.10). Improved methods for finding protein models in electron density maps and the location of errors in these models. *Acta Crystallogr.* A47:110–119.

Kraulis, P. 1991. Molscript: a program to produce both detailed and schematic plots of protein structures. *J. Appl. Crystallogr.* 24:946–950.

Luzzati, V. 1952. Traitement statistique de erreurs dans la determination des structures cristallines. *Acta Crystallogr.* 5:802–810.

Otinowski, Z. 1990. DENZO Data Processing Package. Yale University, New Haven, CT.

Tilton, R. F. J., J. Dwan, and G. A. Pestko. 1992. Effects of temperature on protein structure and dynamics: x-ray crystallographic studies of the protein ribonuclease-A at nine different temperatures from 98 to 320 K. *Biochemistry.* 31:2469–2481.

Tronrud, D. E. 1992. Conjugate direction minimization. *Acta Crystallogr.* A48:912–916.

Tronrud, D. E., L. F. Ten Eyck, and B. W. Matthews. 1987. TNT refinement. *Acta Crystallogr.* A43:489–501.

Yu, B. 1997. X-ray studies of disordered structures in protein crystals. Ph.D. thesis. Brandeis University, Waltham, MA.